Block by Ruthenium Red of the Ryanodine-activated Calcium Release Channel of Skeletal Muscle

JIANJIE MA

Department of Physiology and Biophysics, Case Western Reserve University School of Medicine, Cleveland, Ohio 44106

ABSTRACT The effects of ruthenium red and the related compounds tetraamine palladium (4APd) and tetraamine platinum (4APt) were studied on the ryanodine activated Ca^{2+} release channel reconstituted in planar bilayers with the immunoaffinity purified ryanodine receptor. Ruthenium red, applied at submicromolar concentrations to the myoplasmic side (*cis*), induced an all-or-none flickery block of the ryanodine activated channel. The blocking effect was strongly voltage dependent, as large positive potentials that favored the movement of ruthenium red into the channel conduction pore produced stronger block. The half dissociation constants (K_d) for ruthenium red block of the 500 pS channel were 0.22, 0.38, and 0.62 μM, at +100, +80, and +60 mV, respectively. Multiple ruthenium red molecules seemed to be involved in the inhibition, because a Hill coefficient of close to 2 was obtained from the dose response curve. The half dissociation constant of ruthenium red block of the lower conductance state of the ryanodine activated channel (250 pS) was higher (K_d = 0.82 μM at +100 mV), while the Hill coefficient remained approximately the same (n_H = 2.7). Ruthenium red block of the channel was highly asymmetric, as *trans* ruthenium red produced a different blocking effect. The blocking and unblocking events (induced by *cis* ruthenium red) can be resolved at the single channel level at a cutoff frequency of 2 kHz. The closing rate of the channel in the presence of ruthenium red increased linearly with ruthenium red concentration, and the unblocking rate of the channel was independent of ruthenium red concentrations. This suggests that ruthenium red block of the channel occurred via a simple blocking mechanism. The on-rate of ruthenium red binding to the channel was 1.32×10^9 M^{-1} s^{-1}, and the off-rate of ruthenium red binding was 0.75×10^3 s^{-1} at +60 mV, in the presence of 200 nM ryanodine. The two related compounds, 4APd and 4APt, blocked the channel in a similar way to that of ruthenium red. These compounds inhibited the open channel with lower affinities (K_d = 170 μM, 4APd; K_d = 656 μM, 4APt), and had Hill coefficients of close to 1. The results suggest that ruthenium red block of the ryanodine receptor is due to binding to multiple sites located in the conduction pore of the channel.

Address correspondence to Dr. Jianjie Ma, Department of Physiology and Biophysics, Case Western Reserve University School of Medicine, Cleveland, Ohio 44106.

J. GEN. PHYSIOL. © The Rockefeller University Press · 0022-1295/93/12/1031/26 $2.00
Volume 102 December 1993 1031–1056

INTRODUCTION

In skeletal muscle, excitation of the transverse tubule membranes leads to a transient elevation of the myoplasmic calcium concentration ($[Ca^{2+}]_i$), which is followed by muscle contraction, a process generally referred to as excitation-contraction coupling. This transient increase in $[Ca^{2+}]_i$ is achieved through opening of the Ca^{2+} release channel in the sarcoplasmic reticulum (SR) membrane (Smith, Coronado, and Meissner, 1985). The Ca^{2+} release channel is a large conductance pore, having saturation conductances of ~1 nS for K^+ and ~100 pS for Ca^{2+} (Smith, Imagawa, Ma, Fill, Campbell, and Coronado, 1988). The channel in isolation has two properties resembling a ligand gated channel: (*a*) The conduction pore is relatively nonselective, with a permeability ratio of $P_{Ca}/P_K \sim 6$; and (*b*) the activity of the channel is controlled by physiologically relevant compounds. Myoplasmic Ca^{2+} regulates the opening of the channel through activation and inhibition mechanisms, ATP in the millimolar concentration range enhances the channel activity, and millimolar Mg inhibits the channel activity (Smith, Coronado, and Meissner, 1986).

The use of ryanodine as ligand allowed purification of the ryanodine receptor/Ca^{2+} release channel (Imagawa, Smith, Coronado, and Campbell, 1987; Inui, Saito, and Fleischer, 1987; Lai, Erickson, Rousseau, Liu, and Meissner, 1988), and elucidation of the primary structure of the ryanodine receptor (Takeshima, Nishimura, Matsumoto, Ishida, Kangawa, Minamino, Matsuo, Ueda, Hanaoka, Hirose, and Numa, 1989; Zorzato, Fujii, Otsu, Phillips, Green, Lai, Meissner, and MacLennan, 1990). The purified ryanodine receptors normally exist in a tetrameric complex (Wagenknecht, Grassucci, Frank, Saito, Inui, and Fleischer, 1989; Lai, Misra, Xu, Smith and Meissner, 1989), which is similar to the foot structure identified in the triadic junction of the intact muscle (Franzini-Armstrong, 1970; Block, Imagawa, Campbell, and Franzini-Armstrong, 1988). Planar bilayer recordings identified the ryanodine receptor as the Ca^{2+} release channel (Smith et al., 1988; Lai et al., 1988; Ma, Fill, Knudson, Campbell, and Coronado, 1988; Hymel, Inui, Fleischer, and Schindler, 1988; Williams, 1992). Expression of the cDNA coding for the skeletal muscle ryanodine receptor resulted in a functional Ca^{2+} release channel (Penner, Neher, Takeshima, Nishimura, and Numa, 1989).

Although the ryanodine receptor has been purified and cloned, little was known about the structure of the channel complex, particularly the number of the 560-kD polypeptide that are involved in forming the conduction pore of the channel. The interaction of specific blockers at the single channel level has been widely used to study the structure and function relationship of ion channel gating (Hille, 1992). Drugs of specific actions on the SR Ca^{2+} release channel, like ryanodine (Rousseau, Smith, and Meissner, 1987; Garcia, Avila-Sakar, and Stefani, 1991) and local anesthetics (Endo, 1977; Palade, Dettbarn, Brunder, Stein, and Hals, 1989; Xu, Jones, and Meissner, 1993), have proven to be useful tools in understanding the molecular mechanism of excitation-contraction coupling in skeletal muscle (Fleischer and Inui, 1989; Rios and Pizarro, 1991).

Ruthenium red has a linear structure consisting of three ruthenium (Ru) atoms linked by two oxo-bridges; the Ru atoms serve as a nucleus for a total of 14 amines with a bulk valence of six in acidic solution ($[(NH_3)_5Ru\text{-}O\text{-}Ru(NH_3)_4\text{-}O\text{-}Ru(NH_3)_5]^{6+}$,

Fletcher, Greenfield, Scargill, and Woodhead, 1961). This compound was first used to block mitochondrial Ca^{2+} transport (Moore, 1971). Later it was shown to inhibit Ca^{2+} release from the SR of striated and smooth muscles (Ohnishi, 1979; Miyamoto and Racker, 1982; Antoniu, Kim, Morii, and Ikemoto, 1985; Pampe, Konishi, Baylor, and Somlyo, 1988). It is capable of quenching the efflux of ^{45}Ca from the junctional SR vesicles within milliseconds after addition (Ikemoto, Antoniu, and Meszaros, 1985; Meissner, Darling, and Eveleth, 1986; Sumbilla and Inesi, 1987; Calviello and Chiesi, 1989). Since the early work of Smith et al. (1985), ruthenium red has been widely used as a specific blocker of the SR Ca^{2+} release channel.

The mechanism by which ruthenium red blocks the ryanodine receptors is presently unknown. In ryanodine receptors activated by Ca^{2+} or nucleotides, ruthenium red induces a long term closure that is essentially irreversible on the time scale of the recordings (Smith et al., 1985; 1988). This complete turn-off of the channel made analysis of the blocking mechanism particularly difficult.

Ryanodine is a specific ligand for the Ca release channel, which induced significant conformational changes in the channel structure (Ma, Campbell, and Coronado, 1990). The ryanodine activated channels stayed preferentially in the open configuration under wide range of recording conditions. This long-lived open state permitted a kinetic analysis of the transitions between open and blocked states of the channel induced by ruthenium red. The present work characterized the mechanism of ruthenium red block of the purified ryanodine receptor of rabbit skeletal muscle. The experiments were performed with the ryanodine activated channels, and the analyses were focused on the kinetics of blocking at the single channel level. The strong voltage-dependent and cooperative inhibition of the channel suggests that ruthenium red can physically plug the open channel pore in an all-or-none fashion. Part of the work has appeared in an abstract form (Ma, Kundson, Campbell, and Coronado, 1989).

MATERIALS AND METHODS

Immunoaffinity Purification of the Ryanodine Receptor

Ryanodine receptors were purified from rabbit skeletal muscle by immunoaffinity chromatography (Smith et al., 1988). The proteins were kindly provided by Dr. Kevin P. Campbell and colleagues at the University of Iowa. Briefly, triad membrane fractions were isolated from a young rabbit and the membranes were solubilized with 1% CHAPS detergent. The solubilized membranes were applied to an immunoaffinity column prepared with the purified monoclonal antibody (XA7), specific against the ryanodine receptor. The ryanodine receptor proteins were eluted from the column by KSCN. The purified ryanodine receptor consisted of a single polypeptide of approximate molecular weight 450 kD determined by SDS gel electrophoresis (Imagawa et al., 1987; Smith et al., 1988). Scatchard analysis indicated a maximum binding capacity of B_{max} = 490 pmol/mg protein, and an affinity for ryanodine binding with a K_d = 7 nM.

Planar Bilayer Reconstitution of the Ca^{2+} Release Channel

Planar bilayers were formed across an aperture 0.2 mm in diameter in a delrin cup, with a mixture of brain phosphatidylethanolamine and phosphatidylserine in a weight ratio of 1:1 (Avanti Polar Lipids, Birmingham, AL). The lipids were dissolved in decane (Aldrich Chemical

Co., Milwaukee, WI) at a concentration of 20 to 50 mg lipid/ml decane. Single channel currents were recorded with a List L/M EPC 7 amplifier (List Electronic, DA-Eberstadt, FRG). Currents were filtered through a low-pass Bessel filter (Frequency Devices, Haverhill, MA) at 1.5–5 kHz and digitized at 4–31 kHz. Data acquisition and storage were performed on a PC/AT computer using Keithley-DAS 570 software (Cleveland, OH). All experiments were performed at room temperature (25 ± 3°C).

To study the mechanism of ruthenium red block of the ryanodine receptor, I chose to work on the ryanodine activated channels. 1–3 μg of the purified ryanodine receptor were added to the *cis* solution, that contained 250 mM KCl, 10 μM free Ca^{2+} (buffered with 1 mM EGTA), 10 mM HEPES-Tris (pH 7.4). The *trans* solution was identical to the *cis* solution. In addition, 200 nM ryanodine was always present in both solutions, which allowed recording of the ryanodine activated Ca^{2+} release channel. The ryanodine activated channels were easily identified by their characteristic open times which were longer than those of the normal channels (without ryanodine).

The orientation of the channel in the bilayer was *cis*-myoplasmic/*trans*-luminal SR, in more than 90% of the experiments. This was verified by the asymmetric voltage dependence of the channel gating in the presence of ryanodine. At *cis*-positive potentials, the ryanodine activated channel had faster rate of opening and closing (see Fig. 2). The second independent test was based on the present studies, where the blocking effects of ruthenium red were highly asymmetric (see results, Fig. 9).

Eight different preparations of the immunoaffinity purified ryanodine receptor were tested in the experiments, of which two did not have channel activities. Of the six preparations used, they seemed to give consistent channel activities.

Single Channel Data Analysis and Curve Fitting

The programs for data acquisition and analysis were written by Dr. Hubert Affolter (1986, University of North Carolina, Chapel Hill, NC) in the laboratory of Dr. Roberto Coronado. The initial step in the analysis was to look through the single channel traces under a continuously acquired data file to search for the open and closed levels, using an amplitude histogram analysis. Fits with Gaussian distributions of the open and baseline levels gave the mean value of the open and baseline currents plus their standard deviations. Idealization of the open and closed events was obtained by setting the closed discriminator at two standard deviations above the baseline level and the open discriminator at two standard deviations below the open level (Coronado and Affolter, 1986). The idealized data, containing the duration of each open and closed event and the amplitude of each open event, were stored in an ASCII file. All subsequent analyses were carried out using this ASCII file.

Three basic parameters that define the behavior of the channel were calculated routinely: single channel current amplitude (i_o), open probability of the channel (P_o), and open (τo) and closed (τc) lifetimes of the channel. i_o was obtained from the Gaussian distribution of the open current amplitude. P_o was calculated as the fractional open time during the total recording.

The mean open and closed lifetimes of the channel were obtained from the open time and closed time histograms. Events were binned according to a negative cumulative distribution (Ehrenstein, Blumenthal, Latorre, and Lecar, 1974). The number of exponential terms to best fit the histogram were determined according to the least squares regression analysis. The open time histograms of the normal (in the absence of ryanodine) and ryanodine activated (200 nM ryanodine) channels were best fitted with one exponential term. The closed time histograms of the channels required a fit with two exponential terms (a fast and a slow component).

Curve fitting for the dose response titration of the blockers tested (ruthenium red, tetraamine palladium and tetraamine platinum) were performed with the Sigma Plot program (Jandel Scientific, Corte Madera, CA).

RESULTS

The Ca^{2+} Release Channel Formed by the Purified Ryanodine Receptor

Representative single channel currents through the immunoaffinity purified ryanodine receptor are shown in Fig. 1. The current carrier was symmetrical 250 mM KCl, with the free Ca^{2+} in both solutions buffered at 10 μM with 1 mM EGTA. The use of K^+, instead of Ca^{2+}, as the charge carrier permitted the buffering of Ca^{2+} to any desired level in either solution without affecting the current-voltage relationship. In addition, the monovalent cations (K^+ or Na^+) carry larger currents than the divalent cations (Ca^{2+} or Ba^{2+}), which allows for better time resolution of the single channel currents (Smith et al., 1988).

The channels had large conductances, which exhibited rapid transitions between the open and closed state (Fig. 1 *A*). The amplitude of the single channel currents varied linearly with the holding potential (HP), with a slope conductance of 430 ± 12

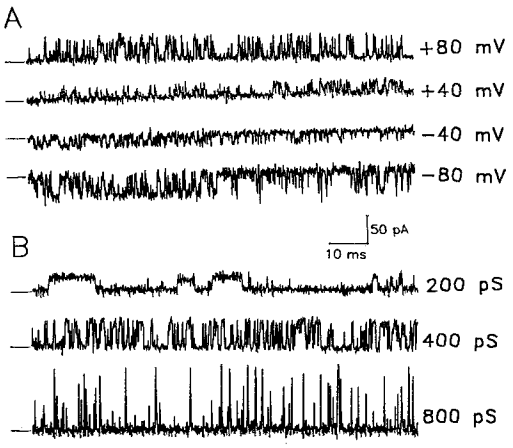

FIGURE 1. K^+ currents through the purified skeletal muscle ryanodine receptor channel. (*A*) The currents at indicated holding potentials were measured with symmetrical 250 mM KCl, 10 μM free Ca^{2+} and 10 mM HEPES-Tris (pH 7.4). The records were filtered at 2 kHz. (*B*) Selected currents at HP = +100 mV were from three different bilayer experiments. The corresponding conductance values were 200, 400, and 800 pS.

pS. The mean open lifetime of the channel was 0.59 ms at HP = +80 mV (Fig. 4). As shown in previous studies (Ma et al., 1988; Smith et al., 1988), the channels formed by the purified ryanodine receptor were similar to the Ca^{2+} release channel found in junctional SR vesicles (Smith et al., 1985), in terms of gating by Ca^{2+}, ATP, pH and particularly the specific effects of ryanodine.

There were differences between the purified ryanodine receptor and the native Ca^{2+} release channel. One such difference is shown in Fig. 1 *B*. These single channel currents were all recorded at HP = +100 mV, but each trace represents separate experiments. The current amplitudes were 20 ± 0.8 pA, 43 ± 1.1 pA, and 78 ± 2.6 pA, corresponding to conductance values of ~200, 400, and 800 pS, respectively. The 400-pS channel was the most frequently observed conductance state (in 41 out of 54 experiments analyzed). Although the native Ca^{2+} release channels (from junctional SR vesicles) exhibit multiple subconductance levels, one rarely observes channels with lower conductance alone in an independent experiment (Ma, Zhou, and Rios, unpublished data).

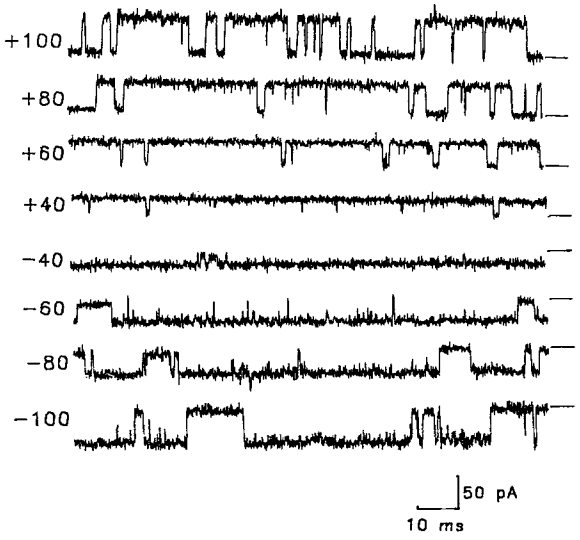

FIGURE 2. Single channel currents of the ryanodine activated channel at various holding potentials. The channel was measured in the presence of 200 nM ryanodine (both *cis* and *trans* solutions). The recording solutions were 250 mM KCl, 10 μM Ca^{2+}, 10 mM HEPES-Tris (pH 7.4). The characteristic long open lifetimes indicated a channel bound to ryanodine. The selected records at the indicated potentials were from the same channel. Marks at right indicate the closed state. The slope conductance of the channel was 509 pS, see Fig. 5.

Gating Properties of the Ryanodine Activated Ca^{2+} Release Channel

Previous studies showed that ryanodine, as a specific ligand for the Ca^{2+} release channel, locked the channel into a long-lived open state and reduced the single channel conductance by 40–50% (Rousseau et al., 1987). The effects of ryanodine are

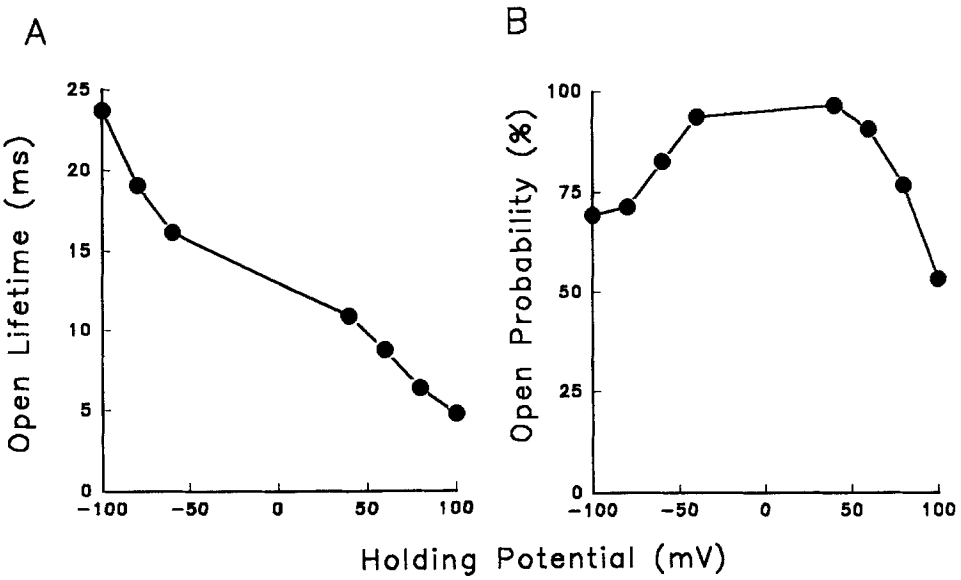

FIGURE 3. Voltage dependence of the ryanodine activated channel. (*A*) The mean open lifetimes (τo) of the ryanodine activated channel decreased monotonically, as the holding potentials became more positive. τo was 24 ms at −100 mV, and τo was 4.6 ms at +100 mV. (*B*) Open probabilities (P_o) of the ryanodine activated channel had a bell shaped dependence on the holding potential. The maximum open probability was 0.94 (at 0 mV).

irreversible and the onset of action is rather slow, due to the slow on-rate of ryanodine binding to the receptor protein (Chu, Diaz-Munoz, Hawkes, Brush, and Hamilton, 1990).

To overcome this slow process, the experiments were started with ryanodine present in the recording solution before the channels were incorporated into the bilayer membranes. Fig. 2 shows records at various membrane potentials with 200 nM ryanodine present in both the *cis* and *trans* solutions. Compared with the normal channel (Fig. 1), the ryanodine activated channel had a long lived open state. The

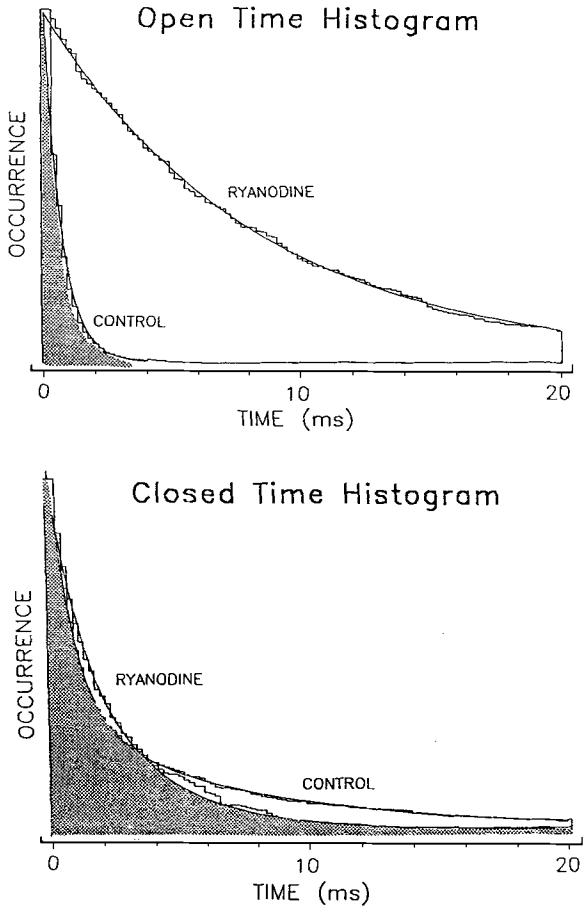

FIGURE 4. Open time and closed time histogram analyses. Events were collected at +80 mV from the same channel before (*control*) and after (*ryanodine*) the onset of the kinetic change induced by ryanodine. The control channel had conductance of ~400 pS, and the ryanodine activated channel had conductance of ~500 pS. The histograms represented 1,745 control events and 574 events of the ryanodine activated channel. The shaded area of each histogram represents the overlap between the control and +ryanodine. The open time histograms (*top*) can be fitted by a single exponential decay, with time constants of τo = 0.59 ± 0.06 ms (*control*) and τo = 8.61 ± 0.54 (*ryanodine*). The closed time histograms had two exponential terms. The corresponding time constants were $\tau c1$ = 1.42 ± 0.21 ms, $\tau c2$ = 8.82 ± 1.20 ms (*control*); and $\tau c1$ = 1.20 ± 0.56 ms, $\tau c2$ = 3.66 ± 0.62 ms (*ryanodine*).

channel had mean open lifetime of 8.6 ms at +80 mV (Fig. 4), which is ~20-fold greater than that observed in the absence of ryanodine. The closed lifetimes of the ryanodine activated channel were also different from the normal channel, but to a lesser extent. Both closed lifetimes exhibit bi-exponential distributions. For the normal channel, $\tau c1$ = 1.42 ms and $\tau c2$ = 8.82 ms, whereas for the ryanodine activated channel, $\tau c1$ = 1.20 ms and $\tau c2$ = 3.66 ms (Fig. 4).

A characteristic voltage dependence of the ryanodine activated channel was observed (Fig. 2). At negative holding potentials, there tended to be silent periods of

channel closings, that resulted in a net reduction of channel open probability (Fig. 3). At positive potentials, the open channels were interrupted by frequent closings, which resulted in a decrease of the channel open lifetime at positive voltages (Fig. 3 *A*). Open probability of the channel as a function of holding potential displayed a bell shaped curve (Fig. 3 *B*). Such voltage dependence was not seen with the normal channels.

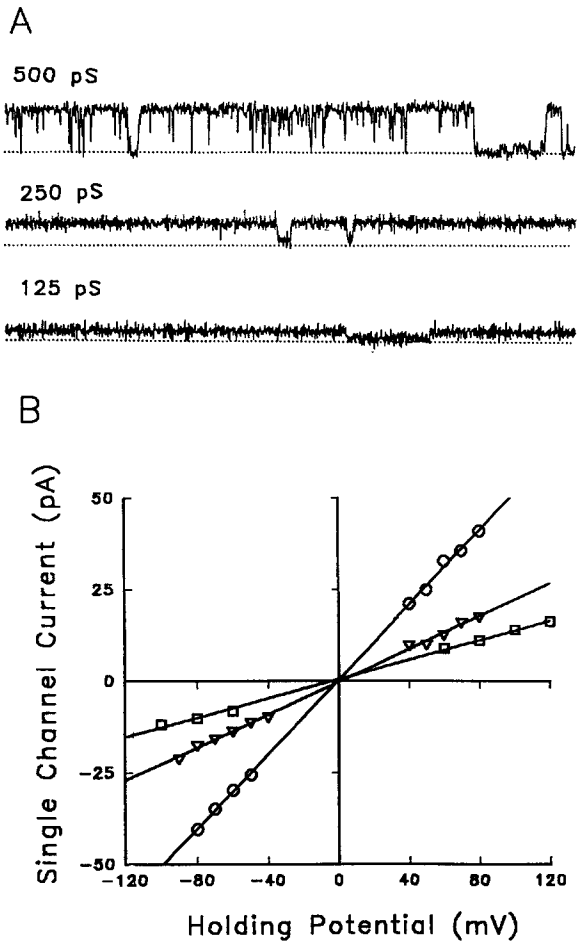

FIGURE 5. Multiple conductance states of the ryanodine activated channel. (*A*) The selected traces (at HP = +80 mV) represent the different conductance states of the ryanodine activated channels, identified in independent experiments. The actual conductance values were given below. (*B*) The circles, triangles, and squares represent the three observed conductance states of the ryanodine activated channel. The current carriers were all 250 mM symmetrical KCl. The corresponding slope conductances were 509 ± 44 pS (*circles*), 224 ± 32 pS (*triangles*) and 132 ± 24 pS (*squares*).

Fig. 2 represents the most frequently observed conductance state of the channel in the presence of 200 nM ryanodine. The slope conductance of the channel was 509 ± 44 pS in 250 mM symmetric KCl (Fig. 5), which is significantly larger than that of the normal channel (430 pS, the most frequently observed state). In the present studies, the reduction in the conductance state of the channel upon binding of ryanodine was not seen in all the experiments, especially starting with the 400 pS normal channel. Sometimes I saw a reduction of conductance from 400 pS to 250 pS after addition of ryanodine, other times I saw an increase of conductance by ~15% (to ~500 pS).

This apparent discrepancy was due to the presence of multiple conductance states associated with the ryanodine activated channel (Fig. 5). Distinct conductances of 500, 250, and 125 pS were observed in independent experiments. The number of observations of each conductance state were summarized in Table I. The 500-pS channel was seen more frequently in experiments initiated with ryanodine already present in the recording solution. The 250-pS channel was the often encountered state after addition of ryanodine to a normal channel in the bilayer. The 125 pS channel was mostly seen with 3 mM Ca^{2+} present in both recording solutions.

TABLE I

Multiple Conductance States of the Ryanodine-Activated Channels

Date	500 pS	250 pS	125 pS
10/87	3	2	0
11/87	1	3	0
12/87	0	1	0
03/88	1	2	1
04/88	2	1	0
05/88	6	1	3
06/88	4	3	1
07/88	8	1	1
08/88	1	0	0
11/88	1	0	0
Totals	27	14	6

Note: of the 27 observations of the 500 pS channel, 14 were pretreated with tyanodine. Of the 14 observations of the 250 pS channel, four were pretreated with ryanodine. Of the six observations of the 125 pS channels, four were measured with 3.5 mM $CaCl_2$ present in both solutions and two were measured with 10 μM free Ca^{2+}.

Voltage Dependent Block of Ryanodine Activated Ca^{2+} Release Channel by Ruthenium Red

The long-lived open state of the ryanodine activated Ca^{2+} release channel allowed for easy identification of the blocking and unblocking events of ruthenium red.

Addition of submicromolar concentrations of ruthenium red to the *cis* solution produced a fast flickery block of the ryanodine activated channel (Fig. 6). Selected records at +60, +80, and +100 mV holding potentials were from one channel with a single conductance state of 500 pS, with symmetrical 250 mM KCl in 10 μM free [Ca^{2+}], 10 mM HEPES-Tris (pH 7.4). The currents were filtered at 2 kHz cutoff frequency. Open times of the reference channel (*top rows*) were interrupted by a relatively small number of closing events, reflecting the slow gating of the ryanodine activated channel. The records in the middle and bottom rows were recorded after addition of 0.5 and 1.2 μM ruthenium red to the myoplasmic side of the channel, respectively. The increased number of fast transitions between open and baseline current levels indicated that ruthenium red blocked the open channel through a fast reaction. Amplitude histograms (not shown) showed that the fast transitions did not result in the formation of new conductance states, other than the open and baseline levels. The block of the open conductance was therefore all-or-none. The records

shown are representative of six experiments performed. The blocking effects of ruthenium red were reversible, as washing out of ruthenium red from the *cis* solution fully recovered the channel activity (two experiments).

Ruthenium red increased the frequency of transitions from open to closed levels (at intermediate concentrations, 0.5 μM) and decreased the tendency of transitions from closed to open states (at high concentrations, 1.2 μM), that contribute to a concentration-dependent decrease in the overall open probability (P_o) of the channel (Fig. 6).

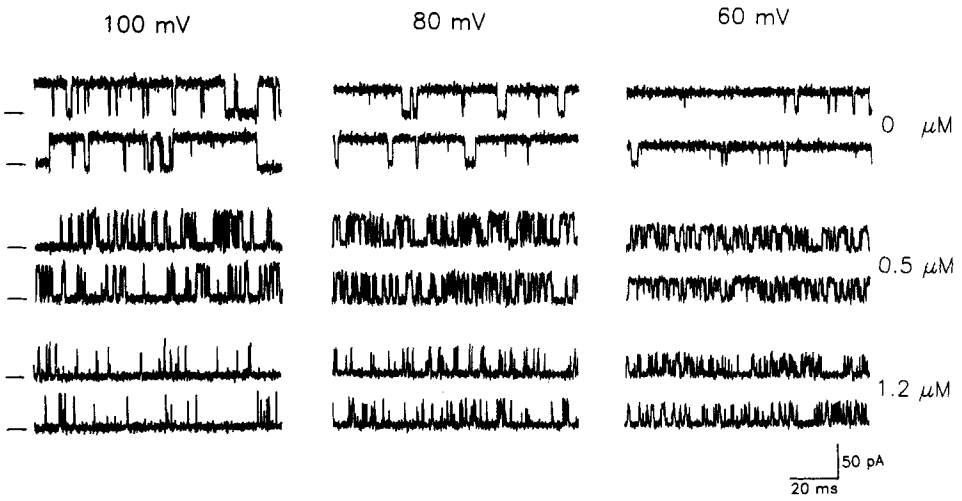

FIGURE 6. Voltage dependent block of the ryanodine activated channels by ruthenium red. The ryanodine activated channels were obtained at a ryanodine concentration of 200 nM (present in both solutions). The single channel currents were measured in symmetrical solutions consisting of 250 mM KCl, 10 mM HEPES-Tris (pH 7.4), and 10 μM Ca^{2+} buffered with 1 mM EGTA. The channel had a slope conductance of 500 pS. The indicated concentration of ruthenium red was added to the *cis* solution, the myoplasmic side of the channel. The represented holding potentials were *cis* minus *trans*.

The blocking events produced by ruthenium red were strongly voltage dependent. Addition of 0.5 μM ruthenium red reduced the open probability of the channel by 80% (from 0.76 to 0.15) at +100 mV, by 60% (from 0.90 to 0.33) at +80 mV, and by 40% (from 0.96 to 0.56) at +60 mV, respectively (Fig. 7 *A*). The voltage-dependent block can also be seen clearly at 1.2 μM ruthenium red, in which the channel had a measurable open probability of 0.25 at +60 mV, while it decreased to essentially zero at +100 mV.

The dose response titration of P_o vs [ruthenium red] is shown in Fig. 7 *A*, at +60 mV (*circles*), +80 mV (*squares*), and +100 mV (*triangles*). The figure showed that ruthenium red blocked the ryanodine activated channel in a narrow concentration range; 0.1 μM ruthenium red did not produce significant block, whereas 2 μM ruthenium red completely inhibited the channel openings. This suggested that the binding reaction of ruthenium red to the channel could be cooperative. The smooth

curves in Fig. 7 *A* were fits of the data according to the Hill equation:

$$P_o = P_{max}/[1 + (X/K_d)^{nH}] \quad (1)$$

where X is the ruthenium red concentration, K_d is the half dissociation constant, n_H is the Hill coefficient, and P_{max} is the open probability of the channel before addition of ruthenium red. The best fit parameters were as follows: K_d = 0.22 ± 0.01 μM, 0.38 ± 0.02 μM, 0.62 ± 0.03 μM and n_H = 2.05 ± 0.08, 2.18 ± 0.13, 2.12 ± 0.15, at +100, +80, and +60 mV, respectively. The half dissociation constants decreased at higher

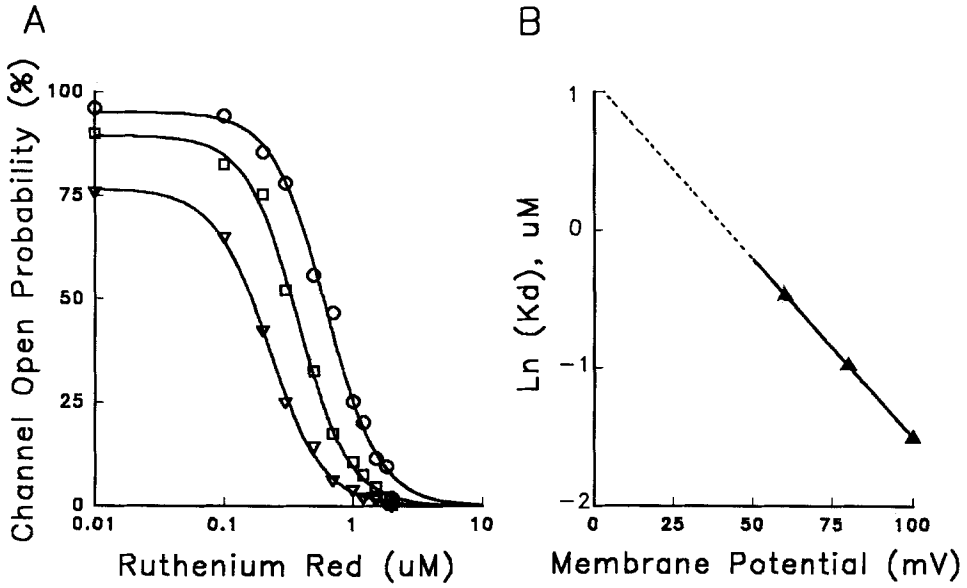

FIGURE 7. Dose-dependent block by ruthenium red of the ryanodine receptor. (*A*) Open probability (P_o) of the channel was measured at each ruthenium red concentration at a given holding potential (*circles*, +60 mV; *squares*, +80 mV; *triangles*, +100 mV). The smooth curves represent the fit according to the Hill equation (Eq. 1). The best fit parameters were K_d = 0.62 ± 0.03 μM, n_H = 2.12 ± 0.15 at +60 mV; K_d = 0.38 ± 0.02, n_H = 2.18 ± 0.13 at +80 mV; and K_d = 0.22 ± 0.01, n_H = 2.05 ± 0.08 at +100 mV. (*B*) Half dissociation constants (K_d) were plotted against the holding potential, on a common log scale. The line through the data points was the fit according to Eq. 2. $K_d(0)$ = 2.93 μM, and δz = 0.79.

holding potentials, confirming the voltage dependent block shown in Fig. 6. The Hill coefficients are all close to n_H = 2, suggesting that at least two ruthenium red molecules are involved in the inhibition of the channel.

The plot of Log(K_d) vs membrane potential appears to have a linear relationship (Fig. 7 *B*). The affinity of ruthenium red block ($K_d(V)$) at a given membrane potential can be described by the following equation:

$$K_d(V) = K_d(0) \exp(-\delta zF/RT) \quad (2)$$

where $K_d(0)$ is the half dissociation constant at 0 mV, and δz the effective valence of

ruthenium red binding to the channel. The extrapolated $K_d(0)$ at 0 mV was 2.9 μM, which is in close agreement with the affinity obtained from [^{3}H]ryanodine binding experiment. Displacement of [^{3}H]ryanodine from the immunoaffinity purified ryanodine receptor by ruthenium red had an IC_{50} of 2–3 μM (Imagawa, Smith, Coronado, and Campbell, 1987). The slope of the fitted line was -0.028 mV^{-1}, this corresponds to a δz value of 0.79. Given the valence of +6 for ruthenium red, the binding sites for ruthenium red should be located a distance equivalent to 0.13 of the membrane field from the myoplasmic side of the channel.

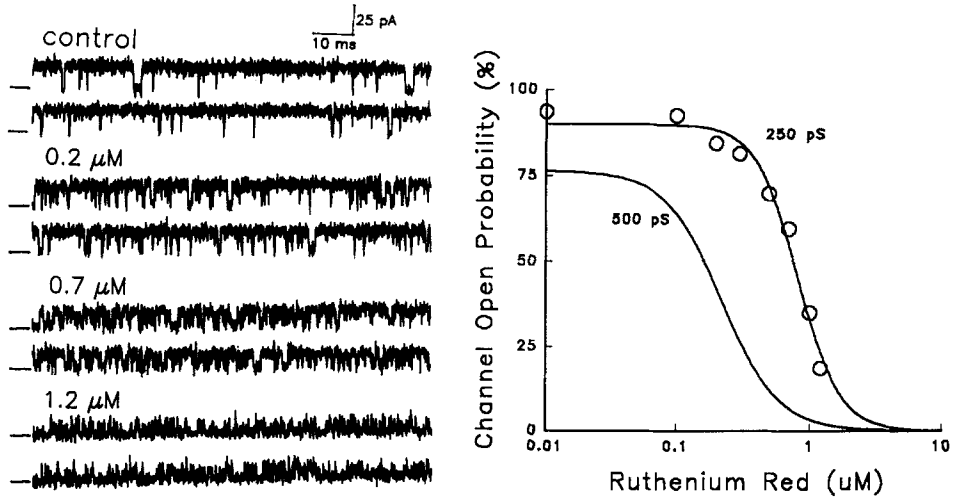

FIGURE 8. Ruthenium red block of the 250-pS conductance channel. The represented single channel currents were at +100 mV holding potential, from a 250-pS channel in the presence of 200 nM ryanodine. The indicated ruthenium red concentrations were added to the *cis* solution. The records shown are representative of two other experiments performed. The dose response curve was fitted according to Eq. 1, with the following parameters: K_d = 0.82 ± 0.04 μM and n_H = 2.77 ± 0.42. The curve without data points was the same as Fig. 7 at +100 mV, for the 500-pS channel.

Ruthenium Red Block of the 250-pS Conductance State

Ruthenium red caused a flickery block of all conductance states of the ryanodine activated channels. Fig. 8 shows selected single channel currents at +100 mV of a 250-pS channel activated by ryanodine before and after exposure to different concentrations of ruthenium red (*left*). The corresponding dose-response curve is shown in the right panel of the same figure. As in the case of 500-pS channels, submicromolar ruthenium red (*cis*) induced a fast block of the 250-pS channel that was concentration-dependent. There was also a clear decrease in channel current at 1.2 μM ruthenium red presumably due to fast unresolved open-closed transitions (at cutoff frequency of 2 kHz).

The major difference between ruthenium red block of the 250-pS channel and the 500-pS channel lies in the dissociation constant (K_d). The concentration dependence of block of the 250-pS channel had a K_d = 0.82 ± 0.04 μM, which is nearly fourfold

larger than that of the 500-pS channel (K_d = 0.22 μM). The best fit Hill coefficient was n_H = 2.74, indicating a cooperative inhibition of ruthenium red of the 250-pS channel. The same dose response curve of the 500 pS channel (at +100 mV) was drawn in Fig. 8, for comparison.

No systematic studies were performed with ruthenium red block of the smallest conductance state (125 pS) of the ryanodine activated channel, because resolution of the fast blocking and unblocking events was more difficult for the smaller currents. In two experiments, higher concentrations of ruthenium red (10 μM) were required to completely inhibit the 125-pS channel. Therefore, the affinity of ruthenium red block of the ryanodine receptor seems to correlate inversely with the conductance state of the channel.

Sidedness of Ruthenium Red Block of the Ryanodine Activated Channel

The blocking effect of ruthenium red was remarkably dependent on the side of the membrane to which it was added. The effect of ruthenium red applied to the *trans* side of the channel is shown in Fig. 9. Single channel traces were taken at −80 mV of a 500 pS ryanodine activated channel. It is clear that trans ruthenium red created a different blocking phenomenon from that of *cis* ruthenium red. Instead of the flickery block that reduces the open probability of the channel (Fig. 7), here ruthenium red attenuated the single channel currents from the luminal SR side of the channel. The overall open probability of the channel was not altered significantly.

The dose response relationship for the effects of ruthenium red applied to the *trans* side is given in Fig. 9 (*right*). The decrease in single channel currents as a function of ruthenium red concentration was fitted by a Hill equation of the following form:

$$I = I_o/[1 + (X/K_d)^{nH}] \quad (3)$$

The best fit parameters were K_d = 0.51 ± 0.07 μM, n_H = 1.32 ± 0.20, and I_o = 35.2 ± 2.0 pA. Thus, *trans* ruthenium red block of the ryanodine activated channel had similar affinity to that of *cis* ruthenium red, but had a Hill coefficient close to 1. This probably indicates that a simple binding site can be approached by ruthenium red from the luminal SR side of the Ca^{2+} release channel.

A voltage dependent blocking effect was also observed for *trans* ruthenium red titration, such that *trans* ruthenium red only reduced the current flow from *trans* to *cis* (at negative potentials), whereas the current flow from *cis* to *trans* (at positive potentials) was not affected (data not shown). The reduction of single channel currents induced by *trans* ruthenium red indicates fast on- and off-rates of ruthenium red binding to the channel. A net negative surface charge exists on the luminal side of the Ca release channel, based on the studies of Tu, Velez, and Fill (1993). This negative charge could concentrate ruthenium red near the binding sites, and be responsible for the observed faster rate of ruthenium red interaction from the *trans* side of the channel.

This highly asymmetric block of the ryanodine receptor by ruthenium red provides an additional way of identifying the orientation of the channel in the bilayer. A normally *cis*-myoplasmic *trans*-luminal SR orientated channel will respond to addition of submicromolar concentration of ruthenium red to the *cis* side with a fast flickery

gating, an inversely orientated channel will respond with a reduction in single channel current amplitude.

Blocking and Unblocking Rates of Ruthenium Red

To kinetically analyze the blocking and unblocking events produced by ruthenium red (applied to the *cis* side) at the single channel level, the open and closed time histograms were constructed. The histograms shown in Fig. 10 represents distributions of open and closed times for a single 500 pS channel in the presence of 0.5 μM and 1.2 μM ruthenium red at +80 mV holding potential. The fit of the exponential distributions was described by the smooth lines running through the binned data. The figure shows that ruthenium red decreased the mean open time in a concentra-

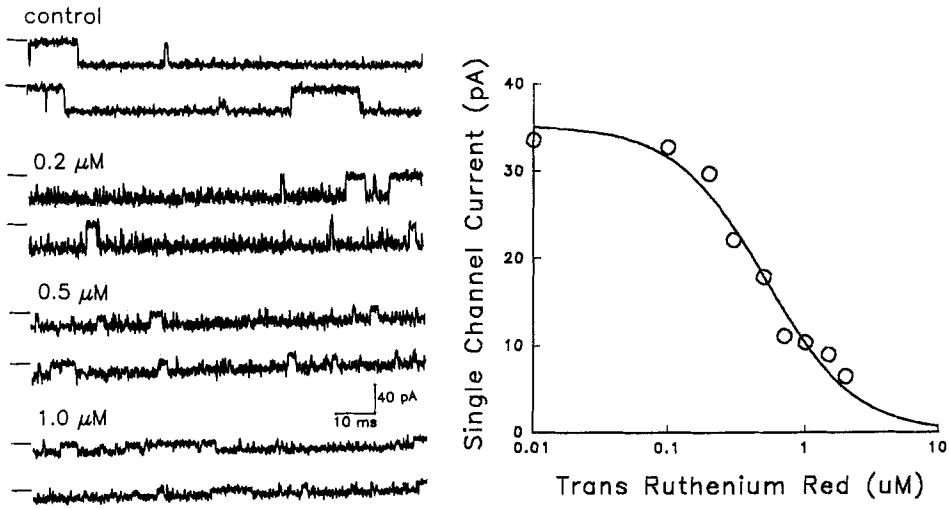

FIGURE 9. Ruthenium red block of the ryanodine activated channel from the luminal SR side. The selected single channel currents were at −80 mV holding potential. The indicated ruthenium red concentrations were added to the *trans* side of the channel. The records shown are representative of three other experiments. The dose response of the single channel currents at a given ruthenium red concentration (*right*) was fitted with Eq. 3. The parameters were: I_o = 35.2 ± 2.0 pA, K_d = 0.51 ± 0.07 μM, and n_H = 1.32 ± 0.20.

tion-dependent manner. The mean open time of the channel before exposure to ruthenium red was 10.3 ms; this was reduced to 1.03 ms and 0.43 ms at 0.5 μM and 1.2 μM ruthenium red, respectively.

A less pronounced effect was observed in the distributions of closed times. The closed time histogram of the reference channels was best fitted by two exponentials, with time constants of τc1 = 1.1 ms and τc2 = 3.1 ms. Both exponentials are drawn separately in Fig. 10 (*top right*) to indicate that ~78% of closed events were fit by the fast closed time, τc1. Addition of ruthenium red changed the distribution of closed times, mainly by changing the proportion of the closed events in τc2. The occurrence of closed events in τc2 was increased from 0.22 to 0.40 with 0.5 μM ruthenium red,

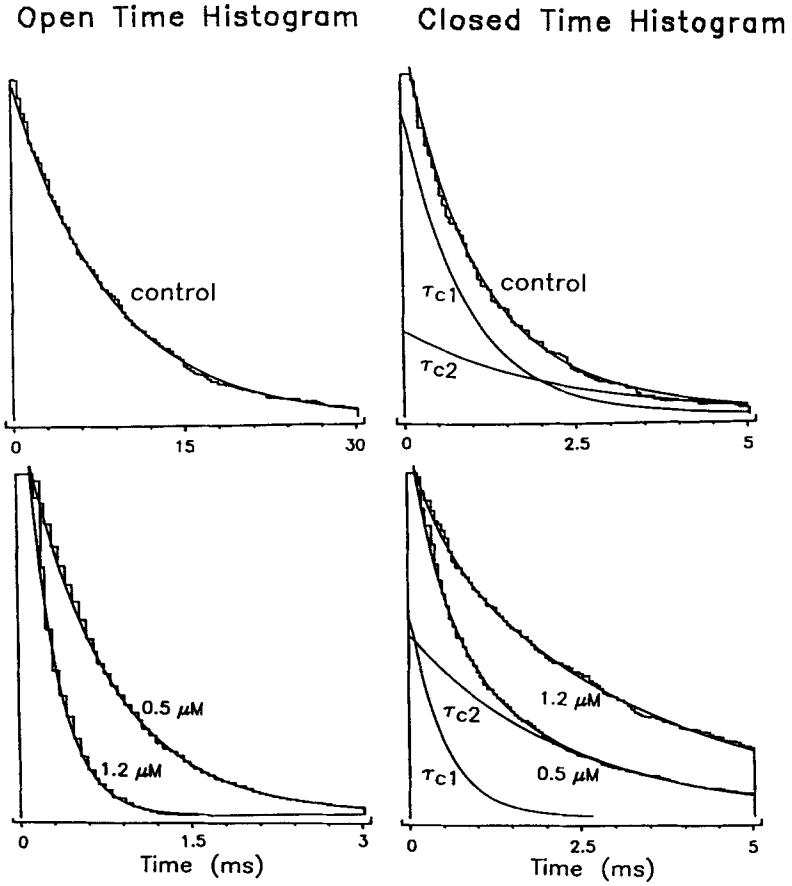

FIGURE 10. Effects of ruthenium red on the open and closed time distributions of the ryanodine activated channel. Distributions of open (*left*) and closed (*right*) times are shown at +80 mV before (control) and after addition of 0.5 μM and 1.2 μM ruthenium red. For comparison, the number of open or closed events was normalized in the y-axis. The number of open events were 244 (*control*), 1575 (+0.5 μM ruthenium red), and 388 (+1.2 μM ruthenium red). The control channels had open time constant of τo = 10.3 ms, and closed time constants of $\tau c1$ = 1.1 ms and $\tau c2$ = 3.1 ms. At 0.5 μM and 1.2 μM ruthenium red, the open time constants were 1.03 ms and 0.43 ms; and closed time constants were $\tau c1$ = 0.8 ms, $\tau c2$ = 2.6 ms, and $\tau c1$ = 1.2 ms, $\tau c2$ = 2.8 ms, respectively.

and 0.86 with 1.2 μM ruthenium red. The time constants of the two exponential distributions did not seem to be altered by ruthenium red. At 0.5 μM ruthenium red, $\tau c1$ = 0.8 ms, $\tau c2$ = 2.6 ms, and $\tau c1$ = 1.2 ms, $\tau c2$ = 2.8 ms at 1.2 μM ruthenium red.

The blocking events induced by ruthenium red did not have a unique exponential component that could be identified and separated from the spontaneous closures of the ryanodine activated channel, because the closed time histograms in the presence of ruthenium red could be adequately fit by two exponential distributions (Fig. 10, *lower right*). A possible explanation is that the unblocking rate of ruthenium red is

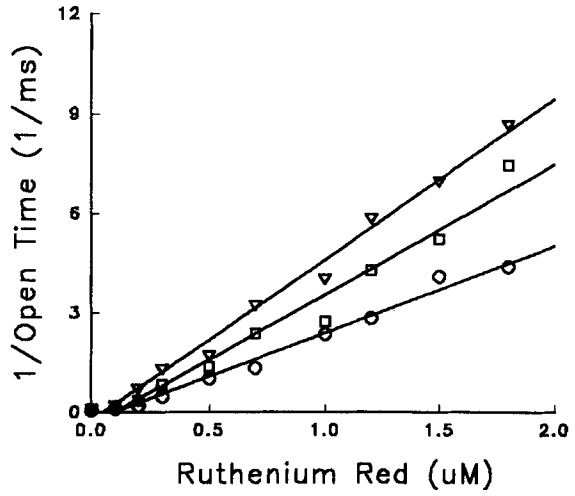

FIGURE 11. Voltage and concentration dependence of open times. The reciprocal of the mean open time was plotted as a function of the ruthenium red concentration at +60 mV (*circles*), +80 mV (*squares*), and +100 mV (*triangles*). The solid lines through the data points were the best fits, with slope factors of 2.63 ± 0.12 μM^{-1} ms^{-1} (*circles*); 3.93 ± 0.24 μM^{-1} ms^{-1} (*squares*), and 4.85 ± 0.17 μM^{-1} ms^{-1} (*triangles*).

numerically similar to $\tau c2^{-1}$, because in the presence of ruthenium red the proportion of closed events in τc2 increased.

The dependence of the open times on ruthenium red concentration is shown in Fig. 11, and that of the closed times is shown in Fig. 12. The three sets of data in both figures correspond to measurements at +60 mV (*circles*), +80 mV (*squares*), and +100

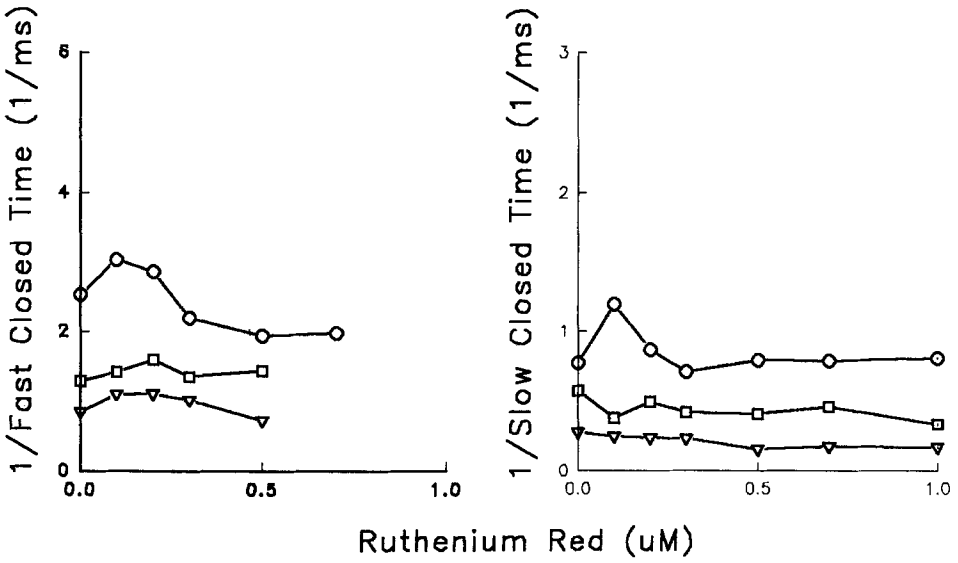

FIGURE 12. Voltage-dependence and concentration-independence of closed times. The reciprocal of the two closed time constants, fast component (τc1) and slow component (τc2), were plotted as a function of the ruthenium red concentration at +60 mV (*circles*), +80 mV (*squares*), and +100 mV (*triangles*). The mean values of 1/τc1 were: 2.58 ± 0.32 ms^{-1} (*circles*); 1.41 ± 0.05 ms^{-1} (*squares*); and 0.95 ± 0.08 ms^{-1} (*triangles*). The mean values of τc2 are: 0.75 ± 0.11 ms^{-1} (*circles*), 0.34 ± 0.05 ms^{-1} (*squares*), and 0.16 ± 0.02 ms^{-1} (*triangles*).

mV (*triangles*). The data were plotted in units of reciprocal milliseconds ($1/\tau o$, $1/\tau c1$, and $1/\tau c2$). The figure showed that the reciprocal open time increased linearly with concentration (Fig. 11), whereas the two closed times did not vary significantly with concentration (Fig. 12).

This concentration-dependence of open times ($1/\tau o$) (Fig. 11), and the concentration-independence of closed times (Fig. 12) suggests that ruthenium red blocks the ryanodine activated channel vis a simple blocking mechanism:

$$C \underset{k_-}{\overset{k_+}{\rightleftharpoons}} O \overset{RR \atop 2k_{on}[x]}{\rightleftharpoons} B \tag{4}$$

The scheme shown above predicts that ruthenium red, by randomly entering and leaving the open channel, should increase the closing rate of the open channel but the lifetime of the blocked state should be unchanged. This is according to the following equations (Neher and Steinbach, 1978):

$$\tau o = 1/(k_- + k_{on}[X]) \tag{5}$$

$$\tau b = 1/k_{off} \tag{6}$$

where k_- is the closing rate in the absence of ruthenium red, k_{on} and k_{off} are first order rate constants for association and dissociation of ruthenium red to the ryanodine receptor.

The slope of the $1/\tau o$ vs [ruthenium red] plot (Fig. 11) should gave an estimation of the on-rate (k_{on}) of ruthenium red binding to the ryanodine receptor. Taking into consideration that two ruthenium red molecules are required to block the open channel (Fig. 7), the on rate should be equal to the slope divided by 2 (the Hill coefficient). The corresponding values of k_{on}, obtained from the linear fit of the data, were 1.32 μM^{-1} ms^{-1}, 1.97 μM^{-1} ms^{-1}, and 2.43 μM^{-1} ms^{-1} at +60, +80, and +100 mV, respectively. These rates were numerically close to the diffusion limited rate of 10^{10} M^{-1} s^{-1} that governs many reactions in solution (Weston and Schwartz, 1972). Estimation of the dissociation rate of ruthenium red from the open channel (k_{off}) can be obtained from the averaged value of $1/\tau c2$ (the slow closed time constant), because the increase in the proportion of the slow closed events ($\tau c2$) seemed to correlate well with the ruthenium red concentration. At +60 mV, k_{off} = 0.75 ms^{-1}. The affinity of ruthenium red binding to the ryanodine activated channel can be calculated as $K_d = k_{off}/k_{on}$ = 0.57 μM, this is in close agreement with the number obtained from the dose-response relationship (Fig. 7).

It should be noted that both the on rate and off rate of ruthenium red binding to the ryanodine activated channel were dependent on the membrane potential. Part of the voltage dependence may be due to the voltage-dependent binding of ryanodine to the purified ryanodine receptor channel, which changes the conformation of the channel structure (Fig. 2).

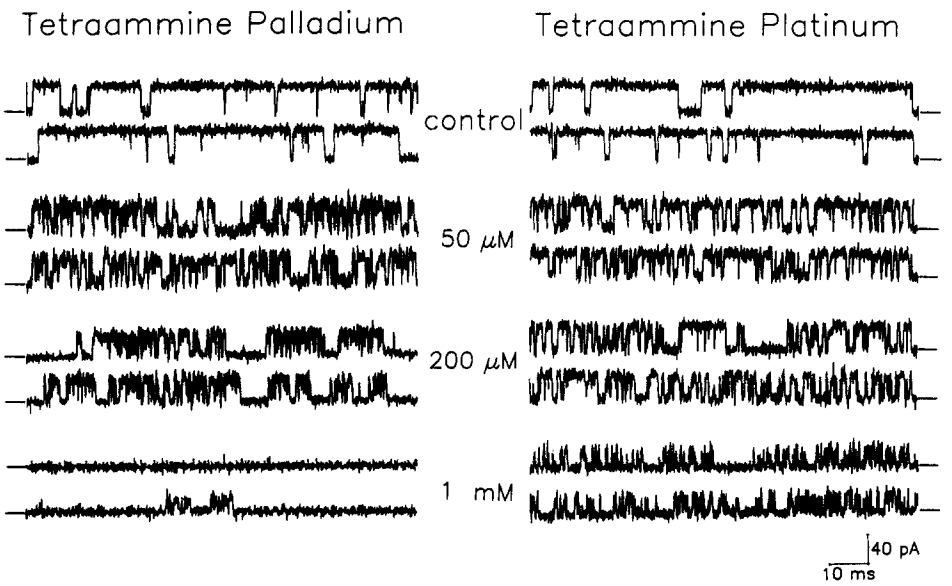

FIGURE 13. Tetraamine palladium (4APd) and tetraamine platinum (4APt) block of the ryanodine activated channel. The effects were tested on the 500-pS ryanodine activated channel. Separate experiments are shown for 4APd and 4APt. The indicated concentrations were added to the *cis* solution. The holding potential was +80 mV. The records shown are representative of two other experiments with 4APd and of three other experiments with 4APt.

Flickery Block by Tetraamine Palladium and Tetraamine Platinum

The complicated structure of ruthenium red, $[(NH_3)_5Ru\text{-}O\text{-}Ru(NH_3)_4\text{-}O\text{-}Ru(NH_3)_5]^{6+}$, may be responsible for the cooperative inhibition of the ryanodine activated channel. To further understand the mechanism of ruthenium red block of

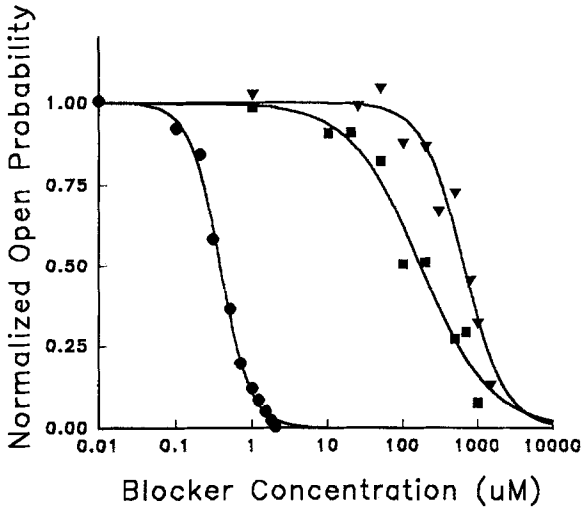

FIGURE 14. Dose dependence of 4APd, 4APt, and ruthenium red block of the ryanodine activated channel. The squares were 4APd titration, the triangles were 4APt titration, and the circles were ruthenium red titration. The corresponding parameters were: K_d = 170.8 ± 44.8 μM, n_H = 0.94 ± 0.18 (*squares*); K_d = 655.7 ± 82.7 μM, n_H = 1.60 ± 0.33 (*triangles*); K_d = 0.377 ± 0.015, n_H = 2.18 ± 0.13 (*circles*).

the channel, Dr. Coronado (my Ph.D thesis advisor) asked me to test compounds with simpler structure. I chose tetraamine platinum $[(NH_3)_4Pt]^{2+}$ (4APt) and tetraamine palladium $[(NH_3)_4Pd]^{2+}$ (4APd) for two reasons, first these compounds contain one end of the ruthenium red molecule, and second pentaamine ruthenium was not available.

Fig. 13 showed that 4APt and 4APd blocked the ryanodine activated channel in a manner similar to that of ruthenium red. Both compounds inhibited the open channel by inducing fast flickery transitions into the closed state of the channel. Similar to ruthenium red, lower doses of both 4APd and 4APt increased closing transitions, while higher doses (1 mM) decreased opening transitions. Millimolar concentrations of both compounds caused a reduction in open channel amplitude, due to the limited bandwidth of recording which left the fast blocking events unresolved. A complete block of channel activity occurred at a concentration of ~ 10 mM (not shown). 4APd seemed to be a more effective blocker of the ryanodine activated channel than 4APt (see records at 1 mM concentration). This could be due to the closer approximity of Pd to Ru, in terms of atomic structure according to the periodic table.

TABLE II

Blocking Parameters of Ruthenium Red and Related Analogues in Ryanodine Receptors of Skeletal Muscle

	Ruthenium red	Tetraamine palladium	Tetraamine platinum
affinity (K_d, μM)	0.38 ± 0.02	170.8 ± 44.8	655.7 ± 82.7
Hill coefficient (n_H)	2.12 ± 0.13	1.04 ± 0.11	1.43 ± 0.53

Note: the parameters were fits according to the Hill equation. The data represented titrations of the 500 pS ryanodine activated channels at holding potential of +80 mV.

Dose-response curves for the block by 4APd (*squares*), 4APt (*triangles*), and ruthenium red (*circles*) are shown in Fig. 14. The concentrations of single pentaamines required to block the channel were in the submillimolar range, rather than in the submicromolar range as in the block by ruthenium red. In addition, both compounds produced an inhibition that was less steeply concentration-dependent than that of ruthenium red. The blocking parameters were summarized in Table II. The Hill coefficients for the block by the single pentaamines were close to one, and the affinity of block by the pentaamines was lower than that of ruthenium red by two orders of magnitude.

DISCUSSION

This study showed that ruthenium red inhibits the ryanodine receptor Ca^{2+} release channel at submicromolar concentrations. Ruthenium red block of the channel was highly asymmetric and strongly voltage dependent. Acting on the ryanodine activated channel, ruthenium red increases the closing rate of the channel while leaving the unblocking rate unchanged. This is consistent with a simple blocking scheme of ruthenium red, working as an open channel blocker.

Multiple Conductance States of the Ryanodine Receptor

The purified ryanodine receptors formed cation selective channels which can exist in multiple conductance states. In the present studies, three distinct conductance states were found in both the normal channel (in the absence of ryanodine) and the ryanodine activated channel (200 nM concentration). The normal channels had conductance values of 800, 400, and 200 pS in 250 mM KCl, with 400 pS state being the most frequently encountered state. The ryanodine activated channels had conductances of 500, 250, and 125 pS, the occurrence of which depends on the experimental procedure and the Ca^{2+} concentration in the recording solution (Table I). The conductance values of the ryanodine activated channels were ~40% less than the corresponding values for the normal channels. This is consistent with the previous work of Rousseau et al. (1987), in which it was shown that ryanodine caused ~40% reduction of the conductance levels of the native Ca^{2+} release channel.

This multiplicity of the conductance states is consistent with the multimeric structure of the ryanodine receptor Ca^{2+} release channel complex (Lai et al., 1989; Wagenknecht et al., 1989). The multiple conductance states of the ryanodine receptor have also been observed in other preparations (Liu, Lai, Rousseau, Jones, and Meissner, 1989). The existence of multiple conductance states of the ryanodine activated channels were reported in more recent studies of Buck, Zimanyi, Abramson, and Pessah (1992).

It should be noted that the observed conductance states were not equally spaced in the present studies. For example, a 600-pS normal channel was never observed in any independent experiments. In addition, most closing transitions were always to baseline level, rather than to the intermediate subconductance level. This would suggest that the 560-kD monomers do not gate independently in forming the channel conduction pore.

Cooperative Inhibition of the Ryanodine Receptor by Ruthenium Red

The fast blocking and unblocking rates of ruthenium red suggests that ruthenium red can easily access the binding sites located on the ryanodine activated channel. The strong voltage dependence of block indicates that the binding sites can sense the voltage changes across the membrane. Therefore, the binding sites must be located within the membrane field, probably in the pore of the channel ($\delta = 0.13$, Fig. 7 *B*). The highly asymmetric effect (*cis* vis *trans* block) suggests that ruthenium red could not permeate through the open channel.

Ruthenium red block of the ryanodine activated channels was cooperative, because a Hill coefficient of 2 was required to account for the dose-dependent inhibition. The actions of ruthenium red on the ryanodine receptor are similar to those of the local anesthetics, such as tetracaine and procaine. Xu et al. (1993) found that the drugs inhibits the open probability of the purified ryanodine receptor Ca^{2+} release channel through cooperative interaction with the channel.

The model presented in Eq. 4 represents an over simplified scheme of ruthenium red block of the channel. Due to the time resolution of the bilayer system, further quantitative analyses were not attempted. The 2 kHz cut-off frequency used in the single channel measurements could only resolve open and closed events with

durations of 0.1 ms or larger (Colquhoun and Sigworth, 1983), the fast blocking events in the submillisecond durations (< 0.1 ms) could not be resolved. Cooperative interaction of ligands with ion channels can be found in many other physiological systems. For example, two acetylcholine molecules are required to activate the cation channels formed by the acetylcholine receptor. Katz and Thesleff (1957) interpreted the cooperative activation of the acetylcholine receptor channel using a model that assumed sequential binding of acetylcholine to two independent binding sites on the channel. Similarly, ruthenium red inhibition of the Ca release channel could occur via independent binding of two ruthenium red molecules to the multiple binding sites on the ryanodine receptor.

$$C \underset{k_-}{\overset{k_+}{\rightleftharpoons}} O \underset{k_{off}}{\overset{2\,k_{on}[x]}{\rightleftharpoons}} B1 \underset{2\,k_{off}}{\overset{k_{on}[x]}{\rightleftharpoons}} B2. \tag{7}$$

The scheme shown above will produce an apparent cooperative inhibition of the open channel by ruthenium red. In addition, it predicts that the blocking events will have two exponential distributions, one of which will have a time constant that varies with ruthenium red concentrations (the closed time of state B1). This component, if exist, is likely to be missed in the bilayer recording system at a cut-off frequency of 2 kHz.

According to the model (Scheme 7), one ruthenium red molecule is sufficient to block the channel, and additional binding of ruthenium red will further keep the channel in the closed state. The two analogues of ruthenium red, 4APd and 4APt, have simpler molecular structure, with only one tetraamine-metal complex. The fact that these two compounds produced similar blocking effect suggests that Ru alone is not sufficient for high affinity block, rather the complexes with the amine groups are important. In addition, 4APd and 4APt block of the channel had Hill coefficients of close to 1 may suggest that the two compounds could have different interactions with the channel than ruthenium red does, or alternatively, the two binding sites for 4APd (or 4APt) could exhibit negative cooperativity, such that only one blocker molecule can reside in the channel at a given time.

Ruthenium red has been used in previous studies of intact muscle fibers to block intracellular Ca^{2+} release (Baylor, Hollingsworth, and Marshall, 1989; Csernoch, Pizarro, Uribe, Rodriguez, and Rios, 1991). It was found that by blocking the SR Ca^{2+} release channel, ruthenium red affected the behavior of the intramembrane charge movement through inhibition of the positive feedback between the SR Ca^{2+} release channel and the voltage sensor (Csernoch et al., 1991). A complication in the interpretation of these results is that a large fraction of the ruthenium red was bound to intracellular organelles. Alternatively, one could use the two analogues (4APd and 4APt) to substitute for ruthenium red. They could prove to be more useful in future cellular studies.

Comparison with Biochemical Binding Assays

The binding characteristics of [^{3}H]ryanodine to the ryanodine receptor have been widely used to monitor the open conformation of the Ca^{2+} release channel (Mitchalak, Dupraz, and Shoshan-Barmatz, 1988; Chu et al., 1991). Factors that favor opening of the Ca^{2+} release channel, such as millimolar ATP and micromolar Ca^{2+},

enhance [^{3}H]ryanodine binding, and those that inhibit the channel activity, such as nanomolar Ca^{2+} and millimolar Mg, decrease [^{3}H]ryanodine binding. Ruthenium red is a specific blocker of the Ca^{2+} release channel because it decreases the [^{3}H]ryanodine binding to the receptor protein at micromolar concentrations. The IC_{50} of ruthenium red displacement of bound [^{3}H]ryanodine from the purified ryanodine receptor was 3 μM (Imagawa et al., 1987), which is very similar to the extrapolated K_d of ruthenium red block of the single ryanodine activated Ca^{2+} release channel (K_d = 2.9 μM at 0 mV, Fig. 7 *B*).

If tetraamine palladium and tetraamine platinum are true blockers of the Ca^{2+} release channel, one would predict that these two compounds should inhibit [^{3}H]ryanodine binding to the receptor. To verify this point, the [^{3}H]ryanodine binding experiments were performed. The experiments were carried out by Dr. Hector Valdivia in the laboratory of Dr. Roberto Coronado. With the ryanodine receptor purified through the sucrose density gradient centrifugation (Lai et al., 1988), he found that 4APd and 4APt were indeed able to displace the bound [^{3}H]ryanodine from the receptor. The measured IC_{50} was 163 and 1,900 μM for 4APd and 4APt, respectively. Therefore, these measurements confirm the single channel studies, which indicate that 4APd and 4APt are true blockers of the Ca^{2+} release channel.

Block of Ryanodine Receptors and Their Relation to Channel Structure

There are currently few clues about the number of 560-kD ryanodine receptor monomers assembled together to form a functional channel. A tetramer is a likely aggregate size because it is a morphological unit recognized in freeze-fractured muscle and in purified preparations (Block, Imagawa, Campbell, and Franzini-Armstrong, 1988). However, it is not known whether tetramers of ryanodine receptors actually represent functional Ca^{2+} channels.

Inferences about a possible oligomeric structure of the channel can be made from an analysis of the conductance states. This has been shown for the channel formed by the dodecapeptide alamethicin (Boheim, 1974; Hall, Vodyanoy, Balasubramanian, and Marshall, 1984). The alamethicin pore exhibits up to six conductance states, each formed by aggregation of dodecapeptide monomers. Transitions to the higher or lower conductance levels occur by uptake or release of one monomer at a time (Boheim, 1974). Given the physical size of the ryanodine receptor monomer and the fact that tetramers survive solubilization in zwitterionic detergents (Lai et al., 1988; Block et al., 1988), it is unlikely that ryanodine receptors are physically pulled in and out of an aggregate to open or close the channel. More likely, it is the loosening or tightening of subunits along their lines of contact in a stable aggregate that makes possible the opening or closing of a large oligomeric channel. In gap junctions, it was suggested that the 30-kD monomers forming part of a stable cylinder-shaped hexamer may render the channel open or closed by a tilt and a slide of each subunit (Unwin and Zampighi, 1980). It is reasonable to assume that the same sliding-cylinder model may apply to the gating of the Ca^{2+} release channel, especially considering the fact that the gating properties of the Ca^{2+} release channel share similarity with those of the gap junctions (Ma et al., 1988).

When conductance states were analyzed under identical bandwidth conditions,

there was an inverse relationship between open lifetime and conductance value for the three frequently encountered states (800, 400, and 200 pS, in 250 mM KCl). The 800-pS channel had the shortest open lifetime of 0.13 ms, and the 200 pS channel had the longest open lifetime of 3.36 ms (Ma, 1989 [Ph.D. thesis]). This observation suggests that each monomer in the tetrameric receptor may have a unitary conductance, and each of the higher conductance levels may represent an integral of the monomeric conductances, resulting from the simultaneous opening of two or more (up to four) monomers.

If there are multiple conductance levels within the ryanodine receptor, how does ruthenium red molecules block all of the states at the same time? Ruthenium red is an open channel blocker based on the concentration dependence of on rate (Fig. 11) and concentration independence of off rate (Fig. 12) of ruthenium red binding to the ryanodine activated channel. Furthermore, ruthenium red and the two related compounds (4APd and 4APt) induced a flickery and complete block (Figs. 6 and 13) of the highest conductance level (500 pS of the ryanodine activated channel). This suggests that all four open monomers in the tetramer were blocked and unblocked simultaneously.

There are two possible explanations for the observed results. First, ruthenium red is a competitive inhibitor of ryanodine binding to the ryanodine receptor protein, based on the biochemical binding assays (Imagawa et al., 1987). Displacement of ryanodine from the receptor protein by ruthenium red led to the inhibition of channel activity. This hypothesis has the problem of accounting for the complete inhibition of channel activity by ruthenium red (Fig. 7), because even in the absence of ryanodine, the channel has a measurable open probability of 10–15% (Ma et al., 1988). Second, if ruthenium red is an open channel blocker, then how can it block all subconductance states simultaneously? The unique structural feature of the ryanodine receptors may provide a possible answer. Tetramers of ryanodine receptors have a characteristic square shape with an apparent central pore (Inui et al., 1987; Lai et al., 1988; Block et al., 1988). The ultra-structural analysis by Wagenknecht et al. (1989) and Radermacher, Wagenknecht, Grassucci, Frank, Inui, Chadwick, and Fleischer (1992) showed that the central channel, originating in the lumen of the SR, branches off into four radial channels leading to the myoplasmic surface of the SR. Although the transmembrane region was not resolved, it is reasonable to think that if a tetramer has one or more transmembrane channels, they would all collect into the central channel before separating into the radial channels. This central channel is likely to be the site where a single blocker can interrupt ion flow in an all-or-none manner. This region appears to be wide enough (5-nm diam, Wagenknecht et al., 1989) to accommodate the 2-nm rod shaped ruthenium red or its smaller analogues (4APd and 4APt). It is interesting that the affinity of ruthenium red block of the ryanodine activated channels correlated inversely with the conductance state of the channel. The channels with higher conductance level is more sensitive to block by ruthenium red. A possible explanation is that the multiconductance pores allow easy access of ruthenium red to the binding sites.

The data presented were partial results of the author's Ph.D. work at the Baylor College of Medicine (1986–1989). I thank Dr. Roberto Coronado for his guidance and encouragement throughout the experiments, Dr. Kevin P. Campbell for providing the purified ryanodine receptor, and Dr. Hector

Valdivia for allowing me to use his [^{3}H]ryanodine binding data with 4APd and 4APt. I also thank Dr. Stephen W. Jones for careful reading of the paper and many suggestions on the models of ruthenium red block.

This work was supported by NIH grants (GM 36852 to R. Coronado and AR 42057 to J. Ma), and Muscular Dystrophy Association Research Grant to J. Ma.

Original version received 10 February 1993 and accepted version received 27 July 1993.

REFERENCES

Antoniu, B., D. H. Kim, M. Morii, and N. Ikemoto. 1985. Inhibitors of Ca^{2+} release from the isolated sarcoplasmic reticulum. I. Ca^{2+} channel blockers. *Biochemica et Biophysica Acta.* 816:9–17.

Baylor, S. M., S. Hollingsworth, and M. W. Marshall. 1989. Effects of intracellular ruthenium red on excitation-contraction coupling in intact frog skeletal muscle fibers. *Journal of Physiology.* 408:617–635.

Block, B. A., T. Imagawa, K. P. Campbell, and C. Franzini-Armstrong. 1988. Structural evidence for direct interaction between the molecular components of the transverse tubule sarcoplasmic reticulum junction in skeletal muscle. *Journal of Cell Biology.* 107:2587–2600.

Boheim, G. 1974. Statistical analysis of alamethicin channels in black lipid membranes. *Journal of Membrane Biology.* 19:277–303.

Buck, E., I. Zimanyi, J. J. Abramson, and I. N. Pessah. 1992. Ryanodine stabilizes multiple conformational states of the skeletal muscle calcium release channel. *Journal of Biological Chemistry.* 267:23560–23567.

Calviello, G., and M. Chiesi. 1989. Rapid kinetic analysis of the calcium-release channels of skeletal muscle sarcoplasmic reticulum: the effect of inhibitors. *Biochemistry.* 28:1301–1306.

Chu, A., M. Diaz-Munoz, M. J. Hawkes, K. Brush, and S. L. Hamilton. 1990. Ryanodine as a probe for the functional state of the skeletal muscle sarcoplasmic reticulum calcium release channel. *Molecular Pharmacology.* 37:735–741.

Colquhoun, D., and F. J. Sigworth. 1983. Fitting and statistical analysis of single-channel records. *In* Single Channel Recording. B. Sakmann and E. Neher, editors. Plenum Publishing Corp., NY. 191–263.

Coronado, R., and H. Affolter. 1986. Insulation of the conduction pathway of muscle transverse tubule calcium channels from the surface charge of bilayer phospholipid. *Journal of General Physiology.* 87:933–953.

Csernoch, L., G. Pizarro, I. Uribe, M. Rodriguez, and E. Rios. 1991. Interfering with calcium release suppresses I_γ, the "hump" component of intramembrane charge movement in skeletal muscle. *Journal of General Physiology.* 97:845–884.

Endo, M. 1977. Calcium release from the sarcoplasmic reticulum. *Physiological Reviews.* 57:71–108.

Ehrenstein, G., R. Blumenthal, R. Latorre, and H. Lecar. 1974. Kinetics of opening and closing of individual excitability-inducing-material channels in a lipid bilayer. *Journal of General Physiology.* 63:707–721.

Fleischer, S., and M. Inui. 1989. Biochemistry and biophysics of excitation-contraction coupling. *Annual Reviews of Biophysics and Biophysical Chemistry.* 18:333–364.

Fletcher, J. M., B. F. Greenfield, H. D. Scargill, and J. L. Woodhead. 1961. Ruthenium Red. *Journal of the Chemical Society.* 2000–2006.

Franzini-Armstrong, C. 1970. Studies of the triad. I. Structure of the junction in frog twitch fibers. *Journal of Cell Biology.* 47:488–499.

Garcia, J., A. J. Avila-Sakar, and E. Stefani. 1991. Differential effects of ryanodine and tetracaine on charge movement and calcium transients in frog skeletal muscle. *Journal of Physiology.* 440:403–417.

Hall, J. E., I. Vodyanoy, T. M. Balasubramanian, and G. R. Marshall. 1984. Alamethicin. A rich model for channel behavior. *Biophysical Journal.* 45:233–247.

Hille, B. 1992. Ionic Channels of Excitable Membranes. Second edition. Sinauer Associates Inc., Sunderland, Massachusetts. 607 pp.

Hymel, L., M. Inui, S. Fleischer, and H. Schindler. 1988. Purified ryanodine receptor of skeletal muscle sarcoplasmic reticulum forms Ca^{2+}-activated oligomeric Ca^{2+} channels in planar bilayers. *Proceedings of the National Academy of Sciences USA.* 85:441–445.

Ikemoto, N., B. Antoniu, and L. Meszaros. 1985. Rapid flow chemical quench studies of calcium release from isolated sarcoplasmic reticulum. *Journal of Biological Chemistry.* 260:14096–14100.

Imagawa, T., J. S. Smith, R. Coronado, and K. P. Campbell. 1987. Purified ryanodine receptor from skeletal muscle sarcoplasmic reticulum is the Ca^{2+} permeable pore of the Ca^{2+} release channel. *Journal of Biological Chemistry.* 262:16636–16643.

Inui, M., A. Saito, and S. Fleischer. 1987. Purification of the ryanodine receptor and identity with feet structures of junctional terminal cisternae of sarcoplasmic reticulum from fast skeletal muscle. *Journal of Biological Chemistry.* 262:1740–1747.

Katz, B., and S. Thesleff. 1957. A study of the 'desentisization' produced by acetylcholine at the motor end-plate. *Journal of Physiology.* 138:63–80.

Lai, F. A., H. P. Erickson, E. Rousseau, Q. L. Liu, and G. Meissner. 1988. Purification and reconstitution of the calcium release channel from skeletal muscle. *Nature.* 331:315–319.

Lai, F. A., M. Misra, L. Xu, H. A. Smith, and G. Meissner. 1989. The ryanodine receptor-Ca^{2+} release channel complex of skeletal muscle sarcoplasmic reticulum. Evidence for a cooperatively coupled, negatively charged homotetramer. *Journal of Biological Chemistry.* 264:16776–16785.

Liu, Q.-Y., F. A. Lai, E. Rousseau, R. V. Jones, and G. Meissner. 1989. Multiple conductance states of the purified calcium release channel complex from skeletal muscle. *Biophysical Journal.* 55:415–424.

Ma, J., M. Fill, M. Knudson, K. Campbell, and R. Coronado. 1988. Ryanodine receptor is a gap junction-type channel. *Science.* 242:99–102.

Ma, J. 1989. Reconstitution of Ca channels involved in excitation-contraction coupling of skeletal muscle. Ph.D. thesis, Baylor College of Medicine, Waco, TX.

Ma, J., C. M. Knudson, K. P. Campbell, and R. Coronado. 1989. Flickery block of the purified ryanodine receptor by ruthenium red, tetraamine palladium, and tetraamine platinum. *Biophysical Journal.* 55:237*a*. (Abstr.)

Ma, J., K. P. Campbell, and R. Coronado. 1990. Ryanodine induces a conformational change in the sarcoplasmic reticulum Ca^{2+} release channel. *Biophysical Journal.* 57:172a. (Abstr.)

Meissner, G., E. Darling, and J. Eveleth. 1986. Kinetics of rapid Ca^{2+} release by sarcoplasmic reticulum. Effects of Ca^{2+}, Mg^{2+}, and adenine nucleotides. *Biochemistry.* 25:244–251.

Michalak, M., P. Dupraz, V. Shoshan-Barmatz. 1988. Ryanodine binding to sarcoplasmic reticulum membrane. Comparison between cardiac and skeletal muscle. *Biochimica et Biophysica Acta.* 939:587–594.

Miyamoto, H., and E. Racker. 1982. Mechanism of calcium release from skeletal sarcoplasmic reticulum. *Journal of Membrane Biology.* 66:193–201.

Moore, C. L. 1971. Specific inhibition of mitochondrial Ca^{2+} transport by ruthenium red. *Biochemical and Biophysical Research Communication.* 42:298–305.

Neher, E., and J. H. Steinbach. 1978. Local anesthetics transiently block currents through single acetylcholine receptor channels. *Journal of Physiology.* 277:153–176.

Ohnishi, S. T. 1979. Calcium induced calcium release from fragmented sarcoplasmic reticulum. *Journal of Biochemistry.* 86:1147–1150.

Palade, P., C. Dettbarn, D. Brunder, P. Stein, and G. Hals. 1989. Pharmacology of calcium release from sarcoplasmic reticulum. *Journal of Bioenergetics and Biomembrane.* 21:295–320.

Pampe, P. C., M. Konishi, S. M. Baylor, and A. P. Somlyo. 1988. Excitation-contraction coupling in skeletal muscle fibers injected with the $InsP_3$ blocker, heparin. *Federation of European Biochemical Societies Letters.* 235:57–62.

Penner, R., E. Neher, H. Takeshima, S. Nishimura, and S. Numa. 1989. Functional expression of the calcium release channel from skeletal muscle ryanodine receptor cDNA. *Federation of European Biochemical Society Letters.* 259:217–221.

Radermacher, M., T. Wagenknecht, R. Grassucci, J. Frank, M. Inui, C. Chadwick, and S. Fleischer. 1992. Cryo-EM of the native structure of the calcium release channel/ryanodine receptor from sarcoplasmic reticulum. *Biophysical Journal.* 61:936–940.

Rios, E., and G. Pizarro. 1991. Voltage sensor of excitation-contraction coupling in skeletal muscle. *Physiological Review.* 71:849–908.

Rousseau, E. C., J. S. Smith, and G. Meissner. 1987. Ryanodine modifies conductance and gating behavior of single Ca^{2+} release channel. *American Journal of Physiology.* 253(Cell Physiol. 22):C364–C368.

Smith, J. S., R. Coronado, and G. Meissner. 1985. Sarcoplasmic reticulum contains adenine nucleotide-activated calcium channels. *Nature.* 316:446–449.

Smith, J. S., R. Coronado, and G. Meissner. 1986. Single channel measurements of Ca^{2+} release channels from skeletal muscle sarcoplasmic reticulum: activation by Ca^{2+}, ATP, and modulation by Mg. *Journal of General Physiology.* 88:573–588.

Smith, J. S., T. Imagawa, J. Ma, M. Fill, K. Campbell, and R. Coronado. 1988. Purified ryanodine receptor from rabbit skeletal muscle is the calcium-release channel of sarcoplasmic reticulum. *Journal of General Physiology.* 92:1–26.

Sumbilla, C., and G. Inesi. 1987. Rapid filtration measurements of Ca^{2+} release from cisternal sarcoplasmic reticulum vesicles. *Federation of European Biochemical Societies Letters.* 210:31–36.

Takeshima, H., S. Nishimura, T. Matsumoto, H. Ishida, K. Kangawa, N. Minamino, H. Matsuo, M. Ueda, M. Hanaoka, T. Hirose, and S. Numa. 1989. Primary structure and expression from complementary DNA of skeletal muscle ryanodine receptor. *Nature.* 339:439–445.

Tu, Q., P. Velez, and M. Fill. 1993. Negatively charged vestibule at the lumenal mouth of the sarcoplasmic reticulum calcium release channel. *Biophysical Journal* 64:304*a*. (Abstr.)

Unwin, P. N. T., and G. Zampighi. 1980. Structure of the junction between communicating cells. *Nature.* 283:545–549.

Wagenknecht, T., R. Grassucci, J. Frank, A. Saito, M. Inui, and S. Fleischer. 1989. Three-dimensional architecture of calcium channel/foot structure of sarcoplasmic reticulum. *Nature.* 338:167–170.

Weston, R. Jr., and H. A. Schwartz. 1972. Chemical Kinetics. Prentice-Hall, Englewood Cliffs, NJ. 161 pp.

Williams, A. J. 1992. Ion conduction and discrimination in the sarcoplasmic reticulum ryanodine receptor/calcium release channel. *Journal of Muscle Research and Cell Motility.* 13:7–26.

Xu, L., R. Jones, and G. Meissner. 1993. Effects of local anesthetics on single channel behavior of skeletal muscle calcium release channel. *Journal of General Physiology.* 101:207–233.

Zorzato, F., J. Fujii, K. Otsu, P. Phillips, N. M. Green, F. A. Lai, G. Meissner, and D. MacLennan. 1990. Molecular cloning of cDNA encoding human and rabbit forms of the Ca^{2+} release channel (ryanodine receptor) of skeletal muscle sarcoplasmic reticulum. *Journal of Biological Chemistry.* 256:2244–2256.